Engineered Science
DOI: https://dx.doi.org/10.30919/es914

Modified Layered Double Hydroxide – PEG Magneto-Sensitive Hydrogels with Suitable Ligno-Alginate Green Polymer Composite for Prolonged Drug Delivery Applications

Hafsa Bahaar,[1] S. Giridhar Reddy,[2,*] B. Siva Kumar,[2,*] K. Prashanthi[1] and H. C. Ananda Murthy[3]

Abstract

A new nanocarrier was developed to address the debilitating side effects associated with cancer treatment, specifically for delivering Sorafenib (SF). This nanocarrier utilises biodegradable polymers, which present a promising approach to anti-cancer therapy by enabling controlled drug release and reduced toxicity. The design of the nanocarrier includes Fe_3O_4 nanoparticles, Sodium alginate, Lignosulphonic acid, Polyethylene glycol, SF drug, and a MgAl layered double hydroxide coating. The nanocarrier was extensively characterised using various techniques, including FT-IR, TGA, and FESEM. Notably, the iron oxide nanoparticle (IONP) nanocarrier demonstrated remarkable superiority in the controlled release of SF compared to other variations. The chemical interactions among the components of the nanocarrier significantly contributed to its enhanced stability, as evidenced by thermogravimetric analysis. Furthermore, XRD analysis confirmed the crystalline nature of the final samples. The FESEM images provided visual confirmation of the morphology of the nanocarrier combinations. Additionally, kinetic models verified the sustained release of SF from the composite alginate matrix. These findings collectively highlight the potential of this nanocarrier system as an effective approach for delivering SF drug in cancer treatment while minimising side effects.

Keywords: Sorafenib; Controlled drug delivery; Anti-cancer drug; Sodium alginate; Polyethylene glycol; Lignosulphonic acid; Biopolymers.
Received: 07 April 2023; Revised: 11 June 2023; Accepted: 15 June 2023.
Article type: Research article.

1. Introduction

Sorafenib is the first and only drug approved by the United State Food and Drug Administration to treat hepatocellular carcinoma. It works by inhibiting the activity of several kinases.[1] *In vitro* studies have shown that SF (Sorafenib) tyrosine kinase inhibition activity can decrease the proliferation of tumour cells, particularly by targeting the Rat sarcoma virus/ Rapidly accelerated fibrosarcoma/Mitogen-activated protein kinase pathway and *Receptor tyrosine kinases*. SF can also induce cancer cell death by increasing the production of reactive oxygen species, such as NO and H_2O_2, which cause oxidative damage to DNA, proteins, lipids, and other components of cancer cells.[2] However, SF has some disadvantages, including low bioavailability and non-specific targeting of normal cells. This is a common problem associated with most chemotherapy drugs, as they cannot distinguish between cancer cells and normal cells, leading to numerous side effects, some of which can be life-threatening.[3] A controlled drug delivery (CDD) approach can overcome these issues by releasing a drug at a specific rate to maintain therapeutic concentrations and reduce dosing frequency.[4] To achieve CDD, various drug delivery systems have been developed using carriers such as liposomes, microemulsions, and microspheres.

Recently, nanotechnology has emerged as a promising field for targeted drug delivery, offering potential solutions to many challenges in conventional drug delivery systems. Using nanotechnology, scientists are developing innovative approaches to improve drug delivery efficiency, specificity, nanoparticle formulations, enhanced permeability & retention

[1] *Department of Biotechnology, Ramaiah University of Applied Sciences, Bengaluru, 560054, India.*
[2] *Department of Chemistry, Amrita School of Engineering, Bengaluru, Amrita Vishwa Vidyapeetham -560035, India.*
[3] *Department of Applied Chemistry, School of Natural Science, Adama Science and Technology University, Adama, P.O. Box:1888, Ethiopia.*
**Email:* s_giri@blr.amrita.edu (S. Giridhar Reddy), b_sivakumar@blr.amrita.edu (B. Siva Kumar)

effect, surface modification, and safety. Targeted drug delivery is the ability to selectively deliver therapeutic agents to specific cells, tissues, or organs while minimising their interaction with healthy cells.[5] Among nanotechnology-based drug delivery systems, polymeric systems have gained immense interest for their potential applications in biomedicine.

Biopolymers are gaining increasing attention in biomedical applications due to their inherent properties of biodegradability and biocompatibility. Sodium alginate is a linear anionic polysaccharide composed of two residues, 1,4-linked β-D-Mannuronate and α-L-Guluronate.[6] The biodegradability of sodium alginate offers significant advantages in the field of CDD. As the drug is gradually released, sodium alginate undergoes degradation, resulting in byproducts that are easily absorbed and excreted by the body without any toxic effects.[7] Sodium alginate's use in biomedical applications is also supported by its low immunogenicity, gelation ability, water solubility, and other properties.[6] It is capable of delivering both macromolecular and low-molecular-weight drugs.

Lignosulphonic acid is a byproduct obtained from wood pulp and has gained attention due to its potential applications in several fields. Lignin, a complex three-dimensional polymer, is the second most abundant natural compound after cellulose. It possesses diverse functional groups, including phenolic hydroxyl, aliphatic hydroxyl, and aryl ether, which render it more chemically reactive than other natural polymers.[8]

Polyethylene glycol (PEG) is a hydrophilic and biocompatible polyether of glycol. It is non-ionic, water-soluble, and exhibits low immunogenicity. PEG is frequently employed in nanoparticle coatings due to its ability to reduce drug toxicity and clearance, ultimately enhancing its therapeutic effectiveness. Additionally, PEG aids carrier systems by evading immune recognition through reduced opsonisation, preventing phagocytosis and increasing drug circulation in the bloodstream.[6]

Iron oxide nanoparticles (IONPs) are widely explored in various fields, including drug delivery.[9] Magnetic IONPs are used in cancer drug delivery applications due to their magnetic properties, chemical stability, and non-toxicity. They improve therapeutic efficacy and drug release, minimise long-term systemic toxicity, and increase the drug's bioavailability in the bloodstream. Furthermore, the use of IONPs addresses the major issue of chemotherapy specificity, allowing the drug to target cancer cells using an external magnetic field.[10]

Magnesium-aluminium-layered double hydroxide (MgAl-LDH) is a versatile material with a layered structure derived from magnesium hydroxide. It is formed by replacing some divalent cations with trivalent ones, resulting in a positively charged layered structure balanced by negatively charged anions in the interlayer space.[11] Because of its positive charge, LDH has excellent potential for drug delivery applications, particularly for drugs with a negative charge. This is because the positively charged surface of LDH facilitates adsorption and internalisation across biological membranes, which are negatively charged, without requiring any additional post-processing steps.[12] Furthermore, the hydrophilic microenvironment created by the 2D inorganic layers of LDH is well-suited for anti-cancer drugs, often poorly soluble in water.

Different formulations have been fabricated for CDD of SF, an anti-cancer drug. These include a range of microgels and polymer systems, including PEG, Chitosan, Poly(lactic-co-glycolic acid), *etc*..[13-16]

This study focuses on the controlled release of SF, a promising anti-cancer drug, using a core-shell nanoparticle formulation. The core consists of IONP, coated with Sodium alginate, Lignosulphonic acid, and Polyethylene glycol (PEG). Finally, the core-shell nanoparticles were further coated with MgAl-LDH to enable CDD. The thermal stability of PEG in the core-shell formulation was investigated to understand its behaviour at elevated temperatures. By studying the thermal stability of these materials, we gain insights into their performance and potential applications in fields such as pharmaceuticals, biomaterials, and industrial processes.[17-19] The synthesised core-shell nanoparticles were evaluated for their drug delivery potential in simulated fluid conditions. This study presents a promising approach for developing drug delivery systems based on LDH-coated core-shell nanoparticles for enhanced therapeutic efficacy.

2. Methods

2.1 Materials

The Ferric chloride hexahydrate (MW=270.295 g/mol), Ferrous sulphate ($FeSO_4$) (MW = 151.91 g/mol) were obtained from Loba chemicals, Ammonia solution (25%) (MW = 17.031 g/mol) from Fisher Scientific, Sodium alginate(SA) and Lignosulphonic acid (LS) purchased from Sigma Aldrich, India, Polyethylene glycol (PEG) obtained from s d fine-chem limited, Mumbai, Aluminium nitrate from Qualikem's Fine Chem Pvt, Ltd., Vadodara, Magnesium nitrate was obtained from Loba chemicals, Sorafenib ($C_{21}H_{16}ClF_3N_4O_3$) was obtained as a gift sample, Dimethyl sulfoxide ($(CH_3)_2OS$). For all preparations, distilled water with a conductance of (18.2 ΩM cm^{-1}) was used.

2.2 Procedure

2.2.1 Preparation of SALS, SA/LS/PEG and IONP

Polymer suspensions were prepared in two compositions, as shown in Fig. 1. 2% of SA and LS acid were dissolved in distilled water. (Fig. 1A). 1% of SA and LS (80:20) and 1% of PEG in distilled water (Fig. 1B).

Ferric oxide nanoparticles (IONP) were synthesised via the co-precipitation method. Aqueous solutions of $FeCl_3 \cdot 6H_2O$ and $FeSO_4$ were prepared separately. Both solutions were mixed using a magnetic stirrer at 60 °C, and the volume was up to 50 ml. A few drops of 25% ammonia solution were added under constant stirring for 15 mins until a pH of 9-10 was

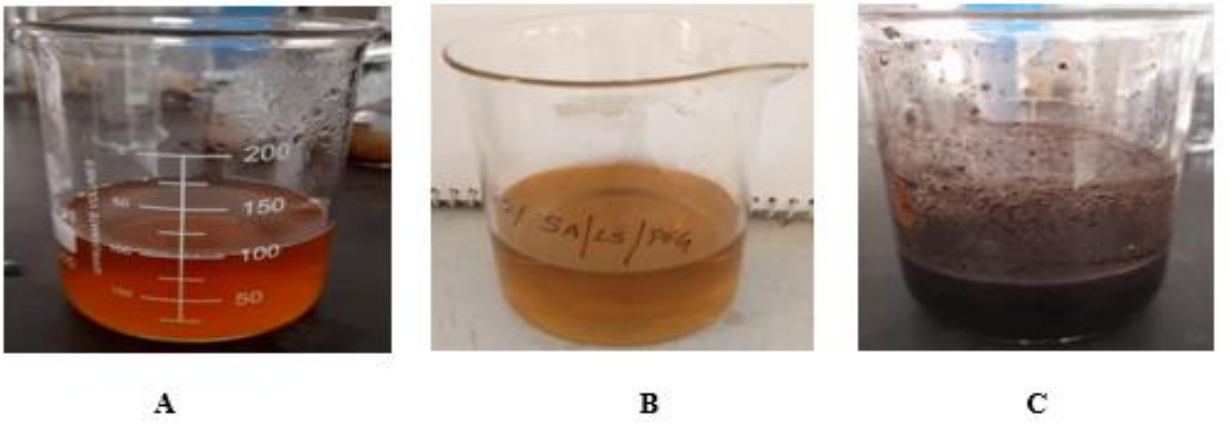

Fig. 1 Synthesis of polymer blends and IONP. (A)2% SA/LS; (B)2% SA/LS/PEG; (C) IONP.

obtained. The temperature was maintained at 40 °C. The appearance of black sediments, as shown in Fig. 1C, indicates the formation of IONP. The sediment was washed thrice using distilled water, followed by its collection.

2.2.2 Preparation of IONP core-shell composite of SF-MgAl-LDH mixtures.

The black precipitate obtained above was suspended in the polymer suspension (SA/LS/PEG and SA/LS/) and heated in a hot air oven at 80 °C for 24 h to obtain the polymer-coated IONP. The black precipitate is then centrifuged at 5000 rpm for 5 mins. Pellet was collected and washed with distilled water to remove unbound polymer.

50 ml of the drug solution was obtained by 1g of Sorafenib dissolved in 50 ml of DMSO. 3 ml of coated IONP/SA/LS/PEG or IONP/SA/LS was added to the Sorafenib (SF) solution. The mixture is stirred on a magnetic stirrer for 24 h at room temperature. Layered double hydroxide (LDH) was synthesised by dissolving magnesium nitrate and aluminium nitrate in 50 ml of distilled water. A few drops of NaOH were added to the mixture while constantly stirring it until pH 9-10 was obtained. MgAl-LDH solution was then dispersed into IONP/SA/LS/PEG/SF and IONP/SA/LS/SF solution and mixed continuously for 15 mins at 40 °C. The sample was then cooled down and centrifuged at 5000 rpm for 5 mins. The sample was then dried in a hot air oven, and the final sample (Table 1) was obtained, as seen in Fig. 2.

Table 1. Sample variants.

Sample code	Final sample
SF1	IONP/SA/LS/SF-MgAl-LDH
SF2	IONP/SA/LS/PEG/SF-MgAl-LDH

The graphical presentation of the encapsulated IONP coated with a polymer, drug solution, and LDH in a sequential order is represented below (Fig. 3).

2.3 Instrumentation

2.3.1 In vitro SF drug release studies

A stock solution of SF was prepared by known concentration by dissolving in DMSO solution. The 6 different dilutions were prepared from the stock solution with concentrations of 0.5, 1, 1.5 and 2 mg of SF drug in 50ml DMSO solution. The above solutions were subjected to UV excitation at 264 nm, and a calibration curve is plotted, as shown in Fig. 4.

The kinetics of SF release from SF2 or SF1 nanocarrier was investigated at two pH solutions. The drug release experiments were carried out at pH levels of 4.6 (acetate buffer)

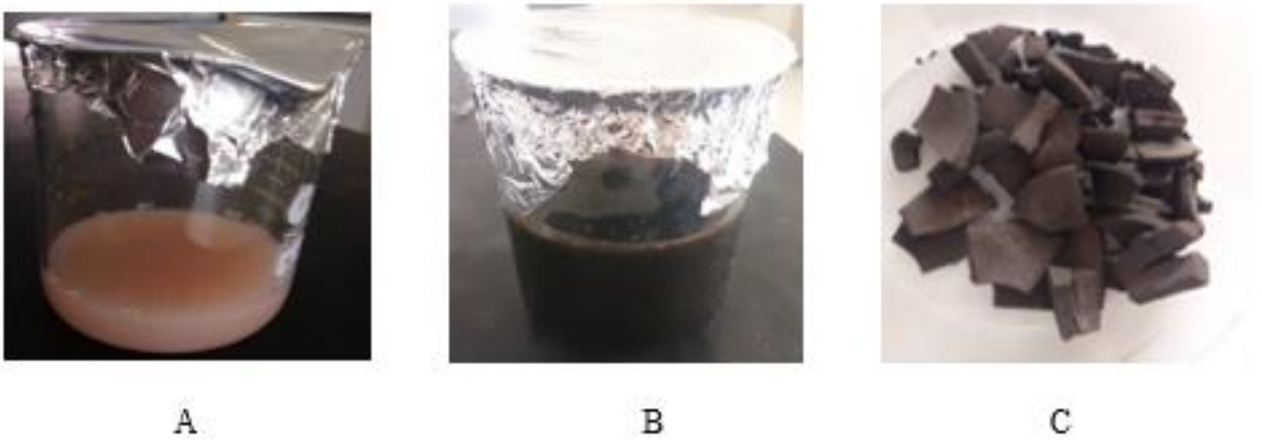

Fig. 2 Synthesis of polymer-coated IONP loaded with the drug. (A) Sorafenib solution in DMSO; (B) Polymer and LDH coated IONP loaded with drug; (C) Final sample (dried).

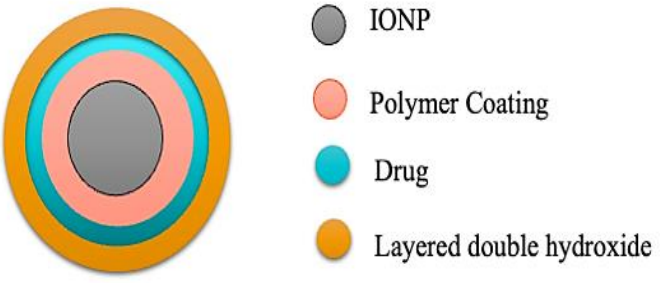

Fig. 3 Schematic diagram of the designed core-shell IONP.

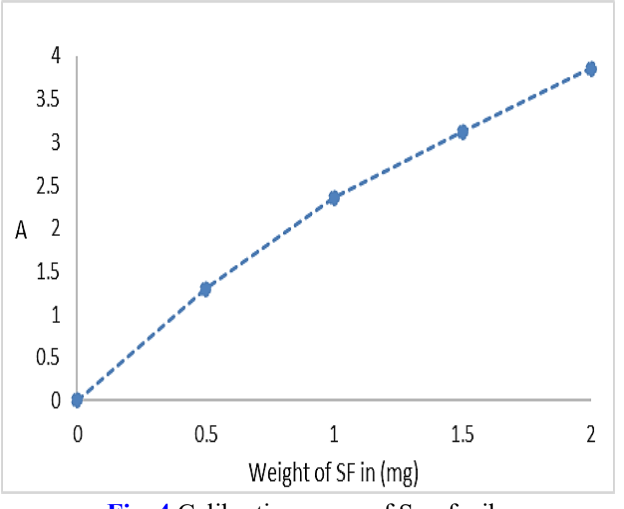

Fig. 4 Calibration curve of Sorafenib.

and 7.4 (PBS), respectively, to replicate the tumour microenvironment and normal cell conditions.[10] The final sample is taken in a beaker containing 50ml buffer solutions. The release of SF from the nanocarrier was measured with UV-Visible Spectrophotometer (Shimadzu 2600) at a range of 185-350nm as the characteristic peak of SF is observed at 264nm.[20] The calibration curve and standard graphs were plotted for each of the two variations to determine the percentage of Sorafenib released.

As shown in Table 2, the different kinetics models are discussed for SF cumulative drug release values using the fit method to understand the drug release mechanism.

Table 2. Reaction mechanism kinetics models.

Models	Equations	Parameters
Zero order	$Q_t = Q_o + K_o t$	K=zero order constant, Q_t, and Q_o are concentrations of drug release at time t and initial
First order	$\ln Q_t = \ln Q_o - K_1 t$	K_1 is first-order kinetics
Higuchi	$Q_t = Q_o + K_H t^{0.5}$	K_H is the Higuchi kinetic constant
Korsmeyer – Peppas	$Q_t = K_{KP} t^n$	K_{KP} is the Korsmeyer - Peppas constant
Kopcha	$Q_t = At^{0.5} + Bt$	A and B are the diffusion and erosion constant

2.3.2 Fourier transform infra-red spectroscopy studies

All the compounds' FT-IR bands were examined to investigate the chemical interactions involved. The spectra were investigated using FTIR (Shimadzu, Model no.206-31000-58, IR Spirit- L). KBr comprising 2-4% by sample weight is used to make the mixed composite pellets. The samples were examined in the 400-4000 cm^{-1} absorption range. The interferogram is created using LAB SOLUTION software and a signal process of 45 scans.

2.3.3 Thermogravimetric analysis

The samples were studied using a Thermo gravimetric analyser (TGA, USA-SDT Q600) for thermal properties. The Universal V4.5A software was used to obtain the readings. Using an alumina pan, this instrument determined the weight change up to 1500° C. The samples were heated at 10° C/min up to 1000° C in a nitrogen gas atmosphere.

2.3.4 X-Ray diffraction studies

The crystallinity of the powdered samples listed in Table 1 was examined using the Rigaku Japan Ultima IV equipment. An X-ray of 1.548 Å wavelength was generated by a Primus 3000 source. The XRD drive system control and data acquisition software was used to process and analyse the signals obtained from the samples, which helped identify the crystal structure and intermolecular distances resulting from intersegmental movement and cross-linking. The diffraction angle of 5 to 90° was utilised for this purpose.

2.3.5 Scanning electron microscope

The Carl Zeiss Germany FESEM is a quick and easy technique for conducting three-dimensional imaging with nanometer precision. By employing a 3D view, polymer samples are repeatedly sliced using an ultramicrotome within the SEM chamber and imaged. The method allows for studying a range of samples' surface morphology and chemical composition.

3. Results and discussion

3.1 *In-vitro* SF drug release studies

The release kinetics of SF drug from SF2 and SF1 nanocarriers were studied at two pH solutions. The drug release studies are performed in pH conditions of 4.6 (acetate buffer) and 7.4 (PBS) to mimic the tumour microenvironment and normal cell conditions, respectively.[10] For the first 10 minutes, there was a considerable variation in the drug release characteristics of both systems at pH 4.6 and 7.4. Overall, the SF drug release was much slower at pH 7.4 compared to the drug's release at pH 4.6. This happens because the drug is more easily released under acidic circumstances. Only a little significant release was observed for 10 mins, and the drug was released in a controlled manner.

Figure 5 indicates the release profiles of SF from the SF2 nanocarrier for five days. The release media used to study the release profile was phosphate-buffered saline and acetate buffer at pH 7.4 and 4.6, respectively. At various times, the

release of the drug into the release media was measured. As seen in the graph, no initial burst was observed, and the drug was released gradually. Within 20 minutes, 3% of the SF was released from SF2 at pH 4.6 and 2.9% at pH 7.4. The release profiles of SF2, at 1 hour, showed a release of 19.2% at pH 4.6 and 4.3% at pH 7.4. As per the literature, it is observed that nanocarrier comprising IONP coated with SA/LS/PEG shows better release as well as ameliorates the initial burst release when compared to the previously reported work by Ebadi et al. (2020). Ebadi et al. developed a nanocarrier for the controlled release of SF, in which IONP formed the core, which was further coated by PEG/ Polyvinyl alcohol. From the results, we can observe that an initial burst of SF was observed; about 83.01% and 82.03% of the SF drug was released from PEG and PVA-coated FONP, respectively, in the first 20mins at the simulated fluid of pH4.8.[10]

As per the drug release data (Fig. 5) of SF2, the maximal quantity of the drug was released within 5 days. At 120 hrs, 99.2% and 23.29% of the drug was observed from SF2 at pH 4.6 and 7.4, respectively. Compared to pH 7.4, the drug release from the sample was dramatically increased at pH 4.6 (acidic environment), resulting in a better drug release efficiency. As a result, the drug release from the nanocarrier was shown to be slower. Because the drug adheres to the surface of IONP, the release of the drug from the nanocarrier is slow. It is determined by the forces required to separate the drug from the nanocarrier.

The surrounding environment's pH is another factor determining the drug's release. In 24hrs, less than 50% of the drug was noticed at pH 4.6 (acidic condition), whereas less than 20% of the drug was released at pH 7.4 (neutral condition).[10,19-22]

Figure 6 indicates the SF release values from the SF1 nanocarrier for two days. At pH 4.6, 43% of the drug was released within 48hrs whereas 10% was released at pH 7.4. After 48hrs, it was noticed that the drug was degraded, and hence we can conclude that there was no release. When we compare the two nanocarriers, we can observe that SF2, which consists of PEG, is more stable, thus making the composite compatible with the drug and enabling its controlled release. Whereas SF1, which does not consist of PEG, is comparatively less compatible with the drug, thus resulting in the release of the drug for a short duration followed by degradation of the drug.

2.2. Fourier Transform Infra-Red studies of IONP coated with Sorafenib drug

FT-IR analysis was performed to confirm the coating of the polymer layer, the SF drug content on the surface of IONPs, and the formation of LDH coating. Fig. 7J shows a characteristic peak of SF at 1652 cm^{-1}, corresponding to -C=O group stretching. The FT-IR spectra of LDH (Fig.7I) display a peak at 836 cm^{-1}, which is associated with the lattice vibration mode of the O-M-O groups. IONP absorbance bands (Fig. 7E) were observed around 578 cm^{-1} and 614 cm^{-1}, indicating the stretching of the Fe-O bond in the Fe_3O_4 crystalline lattice. It is observed that IONP bands were shifted due to their nano size.[10] The FT-IR spectra of SA/LS revealed absorbance peaks at 1045 cm^{-1} (elongation of C-O group), 1419 cm^{-1} (symmetric stretching vibration of COO groups), 1619 cm^{-1} (stretching of carbonyl group) and 654 cm^{-1} (=C-H bend in alkenes).[25-27]

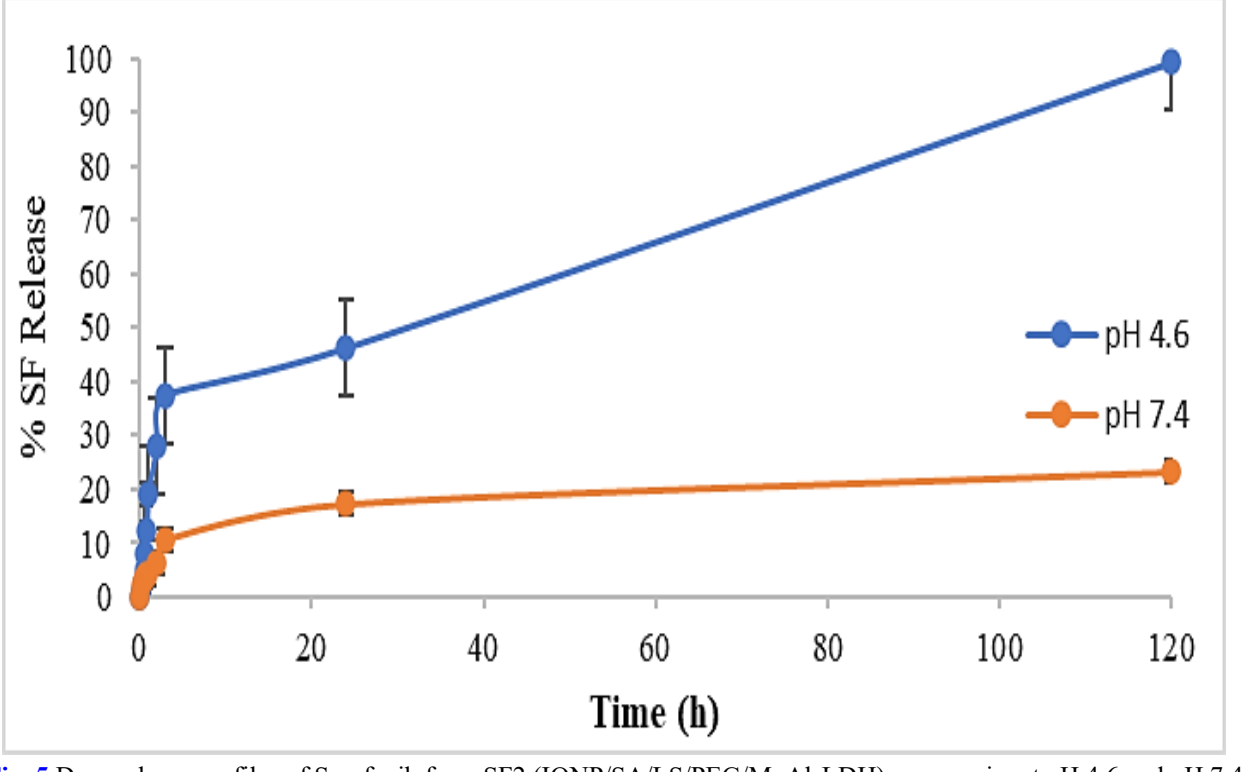

Fig. 5 Drug release profiles of Sorafenib from SF2 (IONP/SA/LS/PEG/MgAl-LDH) nanocarrier at pH 4.6 and pH 7.4

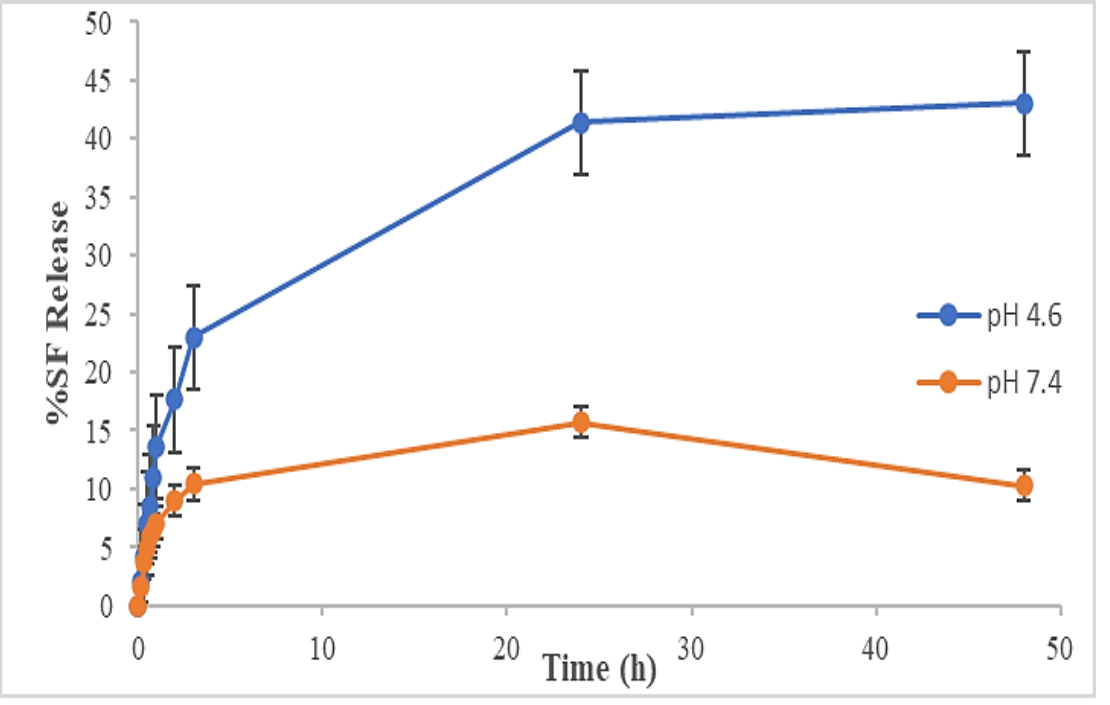

Fig. 6 Drug release profiles of SF from SF1 (IONP/SA/LS/MgAl-LDH) nanocarrier at pH 4.6 and pH 7.4.

The FT-IR spectra of SA/LS and PEG were also compared with SA/LS/PEG blend (as shown in Figs. 7A, 7B and 7C), revealing common peaks. For instance, the SA/LS spectra exhibit a peak at 1619 cm^{-1}, corresponding to carbonyl group stretching. This peak is also present in the SA/LS/PEG blend spectra but with a reduced intensity, confirming the presence of SA/LS in the SA/LS/PEG polymer mixture. Similarly, PEG presents a distinctive peak at 2868 cm^{-1}, corresponding to the vibrations of -CH groups, which is also present in the SA/LS/PEG spectra but with decreased intensity, indicating the presence of PEG in the SA/LS/PEG polymer blend.

To confirm the successful coating of the nanocarrier composite by LDH, FT-IR spectra of IONP, SA/LS/IONP, and SA/LS/PEG/IONP (Figs. 7D, 7E and 7F) were analysed. IONP exhibit a characteristic band at 578 $cm^{-1,}$ indicating the stretching of Fe-O bond in the Fe_3O_4 crystalline lattice. This peak is also observed in the spectra of sample D and sample F, with increased intensities, confirming the presence of IONP in the polymer blend.

FT-IR spectra of Fig. 7G (IONP/SA/LS/MgAl-LDH/SF) and Fig. 7H (IONP/SA/LS/PEG/MgAl-LDH/SF), which were labelled as SF1 and SF2 were analysed to confirm the interactions between the polymers, core, and drug. 1419 cm^{-1} and 1615 cm^{-1} peaks corresponding to the COO group's symmetric stretching vibration and carbonyl group stretching confirm the presence of SA/LS coating. A broad band at 565 cm^{-1} indicates the Fe-O bond's stretching, confirming the IONP's presence in the composite. A peak at 835 cm^{-1} confirms the successful coating of the nanocarrier composite by LDH, which corresponds to the lattice vibration mode of the O-M-O groups. The peak at 1643 cm^{-1}, due to -C=O stretching, is characteristic of SF, confirming the successful loading of the SF drug in the SF1 and SF2 nanocarriers.

3.2 Thermogravimetric analysis

This article discusses the thermal degradation behaviour of IONP that is coated with different polymer compositions and Sorafenib drug. To test the stability of the polymer coatings on IONP, various samples were subjected to heating and measured their weight reduction. We specifically focused on the SALS composition with PEG-coated on IONP.

Figure 8 shows the weight reduction percentage between SF1, SF2, SALS, and SALS/PEG blend. We observed that the biopolymers (SALS and SALS/PEG blend) were less stable compared to the final nanocarrier composition (SF1 and SF2). The SALS and SALS/PEG blend exhibited around 35% weight loss between 210-400 °C.

The TGA results for SF1 showed that the weight reduction on thermal application followed a uniform pattern. This indicated that the shell did not immediately separate from the NP core, which suggested that there was no formation of Fe_3O_4 from IONP. The weight reduction profiles of SF1 and SF2 were similar, indicating no significant difference.

We found that both SF1 and SF2 compositions exhibited IONP stability up to 700 °C and beyond. Overall, the results demonstrate the importance of choosing appropriate polymer coatings for IONP to ensure their stability under thermal conditions.

3.4 X-ray-diffraction studies

Figure 9 illustrates the XRD results of various powdered samples, including IONP, Mg/Al-LDH, SF, SALS, PEG, and co-precipitated synthesised samples. The peaks associated with the iron oxide phase were found in three samples, namely

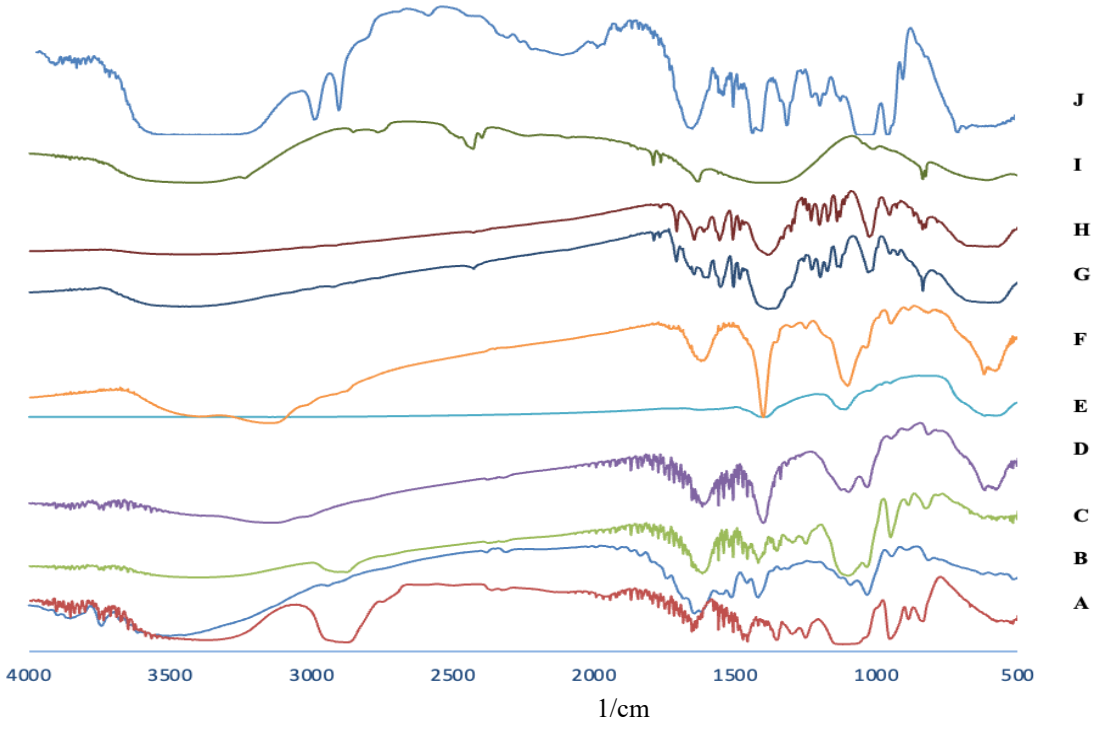

Fig. 7 FT-IR spectra for A) PEG; B) SA/LS; C) SA/LS/PEG; D) IONP/SA/LS/PEG; E) Iron oxide nanoparticles (IONP); F) IONP/SA/LS; G) IONP/SA/LS/MgAl-LDH/SF; H) IONP/SA/LS/PEG/MgAl-LDH/SF; I) MgAl-LDH. J) Sorafenib.

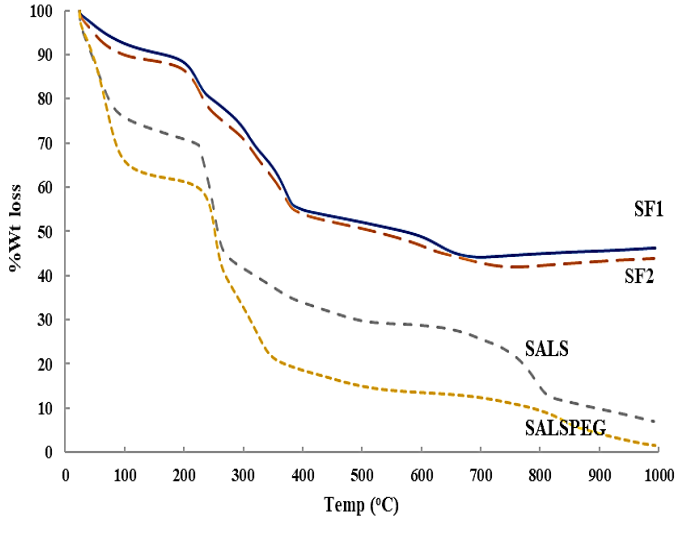

Fig. 8 Thermogravimetric analysis of; A) SF1 (SALS/IONP/LDH/SF); B) SF2 (SALS/PEG/IONP/LDH/SF); C) SALS; D) SALS/PEG.

SF1, SF2, and FeO, with no other subfamily observed. The IONP patterns showed distinct and well-defined peaks.[10] Additionally, the XRD spectra of samples Figs. 9c & 9d at 2θ values of 13, 16, and 19 were identified as SALS and SALS/PEG major peaks, respectively, indicating the presence of these two polymers in the final samples. The final synthesised samples displayed relatively strong peaks associated with MLDH at 2θ values of 23°, 30°, 32° and 39°, and 39° and SF at 2θ values of 10° to 35°, apart from the IONP patterns.[10] The overlapping of SF and MLDH peaks in the synthesised samples of SF1 and SF2 was due to the similarity in their 2θ values. The inset in the figure also showed visible basal spacings from MLDH, which increased when compared to the synthesised samples, indicating the filling of interlayer space of MLDH by SF. Although the synthesised samples could possibly contain a mixture of maghemite and magnetite phases due to interference in the XRD patterns, it couldn't be ruled out.[10] The sharp reflections observed in the pattern of SF1 and SF2 confirmed the crystalline nature of the sample.

3.5 Surface morphology

The FESEM was used to examine the surface morphology of coated magnetic nanoparticles (IONP). The images obtained from the study showed (Fig. 10) that the IONP were spherical with a limited particle size distribution, which can contribute to their stability when used in drug delivery applications. The IONP's high absorbability during germination is due to its energetic and active surface, which allows for quick coating by surface agents, preventing agglomeration and constraining particle growth [10]. The addition of polymers after the production of IONP prevented agglomeration indirectly. However, the washing process during synthesis created agglomerates and secondary structures, which could not be avoided due to interparticle interactions and a magnetic field. Surface coatings partially broke these structures and loaded polymers onto their surface, leading to particle clumping and agglomeration *via* surface attachment during the exchange process.

The results of SEM-EDX analysis showed in Fig. 11 the presence of iron, oxygen, carbon, aluminium, and magnesium

elements in the synthesised IONP. The atomic percentages of iron oxide, oxygen, carbon, aluminium, and magnesium for IONP coated with SALS are 48.5%, 26%, 8%, 4.1%, and 8%, respectively, compared to 49%, 26%, 8%, 4.6%, and 4.6% for IONP coated with SALSPEG. The elements are varied depending on the type of surface coating used, with IONP coated with SALS having slightly different percentages than IONP coated with SALSPEG. The carbon peak was due to polymers, while the peaks for aluminium and magnesium were due to the Mg/Al-LDH phase, and the iron peak was due to the presence of the iron oxide core.

3.6 Release kinetics of SF from SALS and SALS/PEG blends

The study used different kinetic mathematical models, including Higuchi, Zero-order, First-order, and Korsmeyer-Peppas, to investigate the release mechanism of a drug called SF from two formulations, SF1 and SF2, under two different pH conditions (4.8 and 7.4). Table 3, Figs. 5 and 6 show the results of the investigation. Among all the kinetic models, the Korsmeyer-Peppas model had the highest linear correlation coefficient ($R^2 = 0.986$) for SF release at pH 7.4 and 4.8.

The study also looked at the diffusion index (n) value to determine its effect on drug release behaviour. The values of

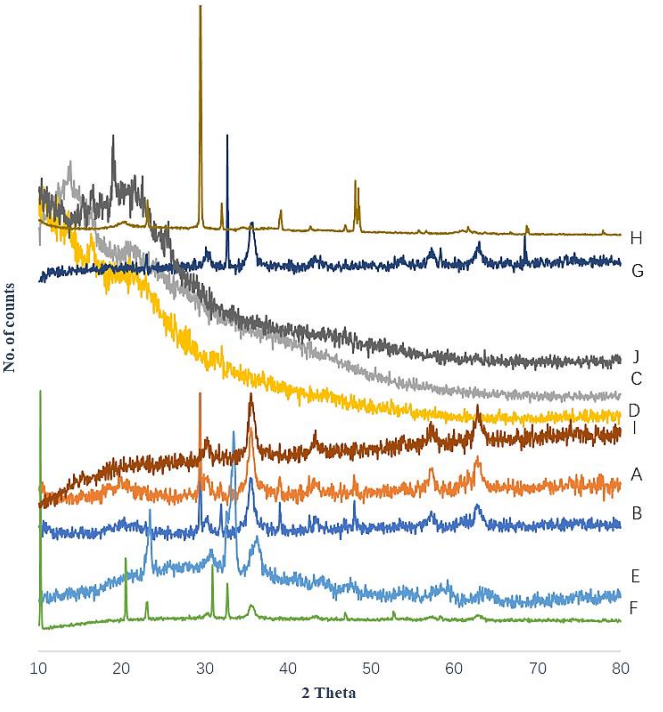

Fig. 9 X-ray diffraction patterns of a) SF1, b) SF2, c) SALS, d) SALSPEG, e) SALSIONP, f) SALSPEGIONP, g) IONP, h) LDH, i) SALS/PEG/IONP/SF, J) SF.

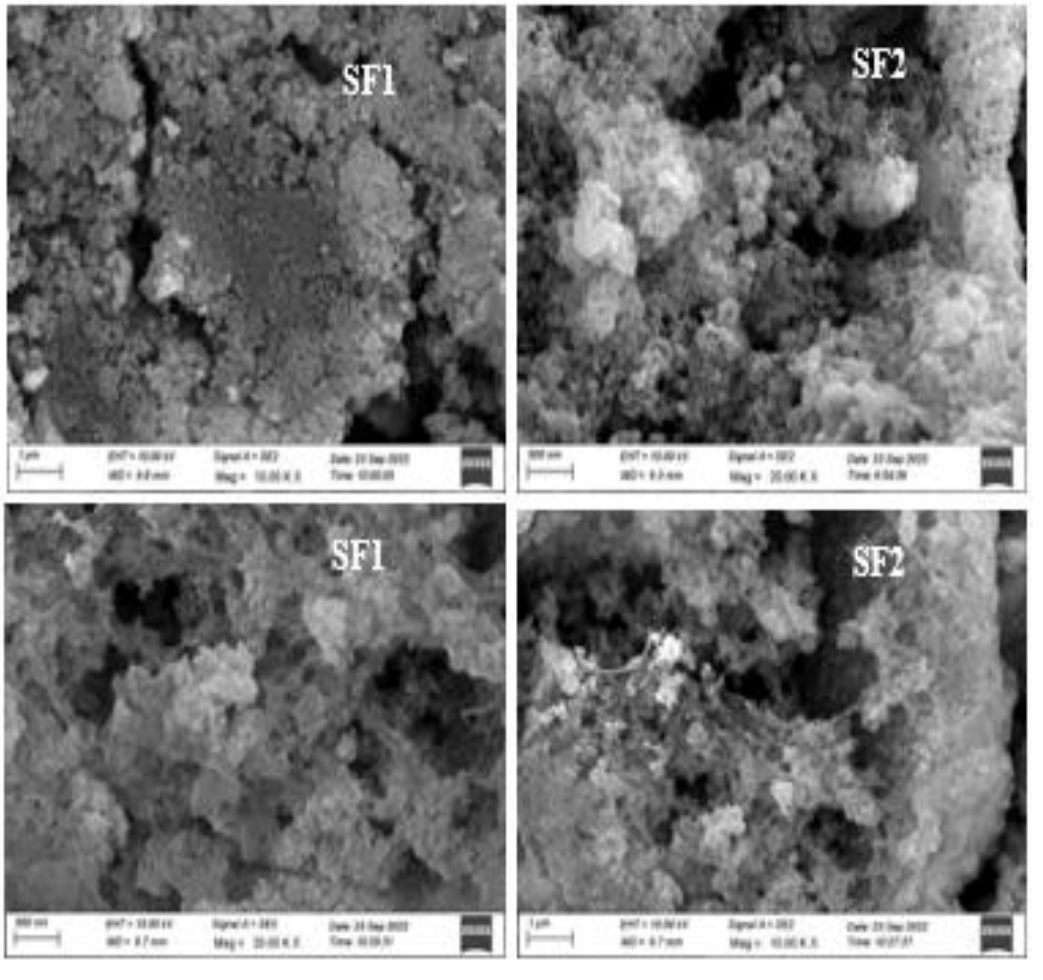

Fig. 10 SEM images of SF1 and SF2 of resolution 1μm and 500 nm.

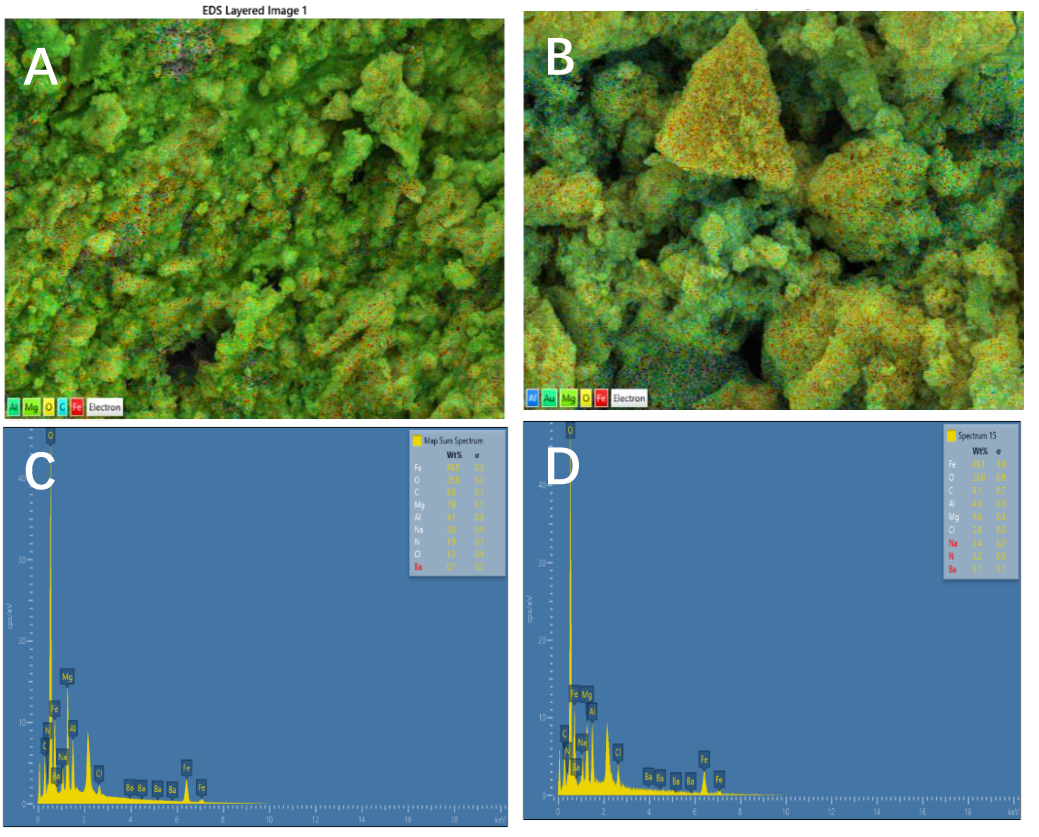

Fig. 11 EDX layered images of (A) SF1; (B) SF2 and SEM-EDX analysis of (C) SF1; (D) SF2.

Table 3. Reaction kinetics parameters.

Model / Samples		Zero order		First order		Higuchi		Korsmeyer–Peppas			Kopcha		
		K	R^2	K1	R^2	K_H	R^2	K_{KP}	n	R^2	A	B	R^2
SALS	pH4.8	2.17	0.55	0.09	0.34	0.62	0.93	12.15	0.35	0.97	9.43	0	0.96
	pH7.4	0.74	0.79	0.06	0.31	3	0.83	6.57	0.45	0.98	4.05	0	0.91
SALS/PEG	pH4.8	1.86	0.77	0.1	0.28	10.2	0.75	15.48	0.37	0.89	11.5	0	0.86
	pH7.4	0.7	0.62	0.08	0.49	3.51	0.93	5.05	0.39	0.97	3.94	0	0.96

'n' were categorised into three cases: Case I ($0<n<0.45$) represented Fickian diffusion, Case II ($0.45<n<0.89$) represented Non-Fickian diffusion, and $n>0.89$ represented the skeletal dissolving process. The study found that the value of $n<0.45$ indicated that the drug release followed Fickian diffusion for controlled drug release.[28,29]

The Higuchi model ($R^2 = 0.93$) was the best fit in both pH media, indicating that the drug is released from blends through diffusion.[26] Additionally, the Kopcha model predicted that the main mechanism of SF release from SF1 and SF2 was diffusion controlled. In both simulated fluids, the diffusion coefficient (A) was greater than the erosion coefficient (B), and the A/B ratio was greater than 1, demonstrating that diffusion was the main mechanism of SF release from both variants.[30-32]

4. Conclusion

In this study, we successfully synthesised two nanocarrier samples, SF1 and SF2, loaded with Sorafenib, a potent anti-cancer drug, to achieve a controlled release and minimise side effects. The results demonstrate that SF1, which comprises PEG in addition to SA/LS, exhibited better stability and more CDD compared to SF2. The IONP-based nanocarrier was characterised using various techniques, including FT-IR, UV spectroscopy, thermogravimetric analysis, XRD, and FESEM, which confirmed the formation of IONP and their coating by the polymers blends and magnesium aluminium layered double hydroxide. The UV spectroscopy results showed a controlled drug release profile from the SF1 nanocarrier, with a release of 19.2% at pH 4.6 and 4.3% at pH 7.4 within the first hour, followed by a sustained release for up to 5 days, where 23.2% of the drug was released in PBS at pH 7.4. Notably, in acetate buffer at pH 4.6, the SF1 nanocarrier exhibited a controlled drug release, with 99.2% of the drug released up to 120 hrs. Our results further confirm the thermal stability of the generated polymers and the crystallinity of the final polymer blend. FESEM analysis also revealed the morphology of the nanocarrier, which showed no

agglomeration due to the immediate coating of IONP by the polymers. Using biodegradable polymers in the nanocarrier enables the controlled release of SF, which is crucial for maintaining therapeutic drug levels over time. SA and LS are natural polymers with significant potential in green materials, particularly in targeting cells and mitochondria. This controlled release mechanism helps optimise the anti-cancer treatment by ensuring a continuous and effective drug concentration at the tumour site while minimising toxicity to healthy tissues. Our findings suggest that the developed polymer blends of SA/LS and SA/LS/PEG with IONP can be an effective nanocarrier for the controlled release of SF and hold great potential for cancer treatment.

Acknowledgement

We sincerely thank all individuals and organisations who have supported us in completing this manuscript. First and foremost, we extend our heartfelt thanks to our research participants, who generously shared their time and experiences with us. We thank the Central Research Institute Facilities from Sri Sathya Sai Institute of Higher Learning, Puttaparthy, India, for TGA and SEM characterisation and the COE-AMGT instrumentation facility from Amrita Vishwa Vidyapeetham, Coimbatore campus for FESEM characterisation. Their support enabled us to conduct this study and provided us with the necessary resources to conduct our research. We also acknowledge the support of the institution where the research was conducted. The resources and facilities provided by the institution were critical in facilitating the research and ensuring its success.

Once again, we express our sincere gratitude to all those who have contributed to this manuscript.

Conflict of Interest

There is no conflict of interest.

Supporting Information

Not applicable.

References

[1] A. A. Abdelgalil, H. M. Alkahtani, F. I. Al-Jenoobi, Sorafenib, *Profiles of Drug Substances, Excipients and Related Methodology*, 2019, **44**, 239-266, doi: 10.1016/bs.podrm.2018.11.003.

[2] R. Coriat, C. Nicco, C. Chéreau, O. Mir, J. Alexandre, S. Ropert, B. Weill, S. Chaussade, F. Goldwasser, F. Batteux, Sorafenib-induced hepatocellular carcinoma cell death depends on reactive oxygen species ProductionIn VitroandIn vivo, *Molecular Cancer Therapeutics*, 2012, **11**, 2284-2293, doi: 10.1158/1535-7163.mct-12-0093.

[3] G. Alessandri, V. Coccè, F. Pastorino, R. Paroni, M. Dei Cas, F. Restelli, B. Pollo, L. Gatti, C. Tremolada, A. Berenzi, E. Parati, A. Teresa Brini, G. Bondiolotti, M. Ponzoni, A. Pessina, Microfragmented human fat tissue is a natural scaffold for drug delivery: potential application in cancer chemotherapy, *Journal of Controlled Release*, 2019, **302**, 2-18, doi: 10.1016/j.jconrel.2019.03.016.

[4] R. Langer, New methods of drug delivery, *Science*, 1990, **249**, 1527-1533, doi: 10.1126/science.2218494.

[5] P. Utreja, S. Jain, A. K. Tiwary, Novel drug delivery systems for sustained and targeted delivery of anti-cancer drugs: current status and future prospects, *Current Drug Delivery*, 2010, **7**, 152-161, doi: 10.2174/156720110791011783.

[6] V. Taghipour-Sabzevar, T. Sharifi, M. M. Moghaddam, Polymeric nanoparticles as carrier for targeted and controlled delivery of anticancer agents, *Therapeutic Delivery*, 2019, **10**, 527-550, doi: 10.4155/tde-2019-0044.

[7] N. K. Sachan, S. Pushkar, A. Jha, A. Bhattcharya, Sodium alginate: the wonder polymer for controlled drug delivery, *Journal of Pharmacy Research*, 2009, **2**, 1191-1199. https://www.scinapse.io/papers/2738741443

[8] S. Gonçalves, J. Ferra, N. Paiva, J. Martins, L. H. Carvalho, F. D. Magalhães, Lignosulphonates as an alternative to non-renewable binders in wood-based materials, *Polymers*, 2021, **13**, 4196, doi: 10.3390/polym13234196.

[9] T. Vangijzegem, D. Stanicki, S. Laurent, Magnetic iron oxide nanoparticles for drug delivery: applications and characteristics, *Expert Opinion on Drug Delivery*, 2019, **16**, 69-78, doi: 10.1080/17425247.2019.1554647.

[10] M. Ebadi, S. Bullo, K. Buskara, M. Z. Hussein, S. Fakurazi, G. Pastorin, Release of a liver anticancer drug, sorafenib from its PVA/LDH- and PEG/LDH-coated iron oxide nanoparticles for drug delivery applications, *Scientific Reports*, 2020, **10**, 21521, doi: 10.1038/s41598-020-76504-5.

[11] S. Saha, S. Ray, R. Acharya, T. K. Chatterjee, J. Chakraborty, Magnesium, zinc and calcium aluminium layered double hydroxide-drug nanohybrids: a comprehensive study, *Applied Clay Science*, 2017, **135**, 493-509, doi: 10.1016/j.clay.2016.09.030.

[12] Y. Kuthati, R. K. Kankala, C.-H. Lee, Layered double hydroxide nanoparticles for biomedical applications: current status and recent prospects, *Applied Clay Science*, 2015, **112-113**, 100-116, doi: 10.1016/j.clay.2015.04.018.

[13] Y. Su, K. Wang, Y. Li, W. Song, Y. Xin, W. Zhao, J. Tian, L. Ren, L. Lu, Sorafenib-loaded polymeric micelles as passive targeting therapeutic agents for hepatocellular carcinoma therapy, *Nanomedicine*, 2018, **13**, 1009-1023, doi: 10.2217/nnm-2018-0046.

[14] T. M. Caputo, A. Aliberti, A. M. Cusano, M. Ruvo, A. Cutolo, A. Cusano, Stimuli-responsive hybrid microgels for controlled drug delivery: Sorafenib as a model drug, *Journal of Applied Polymer Science*, 2021, **138**, 50147, doi: 10.1002/app.50147.

[15] N. Tahir, A. Madni, W. Li, A. Correia, M. M. Khan, M. A. Rahim, H. A. Santos, Microfluidic fabrication and characterization of Sorafenib-loaded lipid-polymer hybrid nanoparticles for controlled drug delivery, *International Journal of Pharmaceutics*, 2020, **581**, 119275, doi: 10.1016/j.ijpharm.2020.119275.

[16] U. Ruman, K. Buskaran, G. Pastorin, M. J. Masarudin, S. Fakurazi, M. Z. Hussein, Synthesis and characterization of chitosan-based nanodelivery systems to enhance the anticancer effect of sorafenib drug in hepatocellular carcinoma and colorectal adenocarcinoma cells, *Nanomaterials*, 2021, **11**, 497, doi: 10.3390/nano11020497.

[17] D. Rana, K. Bag, S. N. Bhattacharyya, B. M. Mandal, Miscibility of poly(styrene-co-butyl acrylate) with poly(ethyl methacrylate): existence of both UCST and LCST, *Journal of Polymer Science Part B: Polymer Physics*, 2000, **38**, 369-375, doi: 10.1002/(SICI)1099-0488(20000201)38:3<369::AID-POLB3>3.0.CO;2-W.

[18] C. Bhattacharya, N. Maiti, B. M. Mandal, S. N. Bhattacharyya, Thermodynamic characterization of miscible blends from very similar polymers by inverse gas chromatography. The poly(ethyl acrylate)-poly(vinyl propionate) system, *Macromolecules*, 1989, **22**, 4062-4068, doi: 10.1021/ma00200a043.

[19] D. Rana, B. M. Mandal, S. N. Bhattacharyya, Analogue calorimetry of polymer blends: poly(styrene-co-acrylonitrile) and poly(phenyl acrylate) or poly(vinyl benzoate), *Polymer*, 1996, **37**, 2439-2443, doi: 10.1016/0032-3861(96)85356-0.

[20] O. Şenol, Rapid determination and validation of sorafenib via UV-Vis method in pharmaceutical formulations, *Balıkesir Sağlık Bilimleri Dergisi*, 2018, **7**, 87-92. https://dergipark.org.tr/en/pub/balikesirsbd/issue/38838/444872.

[21] Khalilov, Rovshan. "A Comprehensive Review Of Advanced Nano-Biomaterials In Regenerative Medicine And Drug Delivery, *Advances in Biology & Earth Sciences*, 2023, **8**, 5-18. http://jomardpublishing.com/UploadFiles/Files/journals/ABES/V8N1/Khalilov.pdf.

[22] A. Eftekhari, C. Kryschi, D. Pamies, S. Gulec, E. Ahmadian, D. Janas, S. Davaran, R. Khalilov, *Natural and synthetic nanovectors for cancer therapy*, Nanotheranostics, 2023, **7**, 236-257, doi: 10.7150/ntno.77564.

[23] M. Ebadi, K. Buskaran, S. Bullo, M. Z. Hussein, S. Fakurazi, G. Pastorin, Drug delivery system based on magnetic iron oxide nanoparticles coated with (polyvinyl alcohol-zinc/aluminium-layered double hydroxide-sorafenib), *Alexandria Engineering Journal*, 2021, **60**, 733-747, doi: 10.1016/j.aej.2020.09.061.

[24] Aashli, S. G. Reddy, B. Siva Kumar, K. Prashanthi, H. C. A. Murthy, Fabricating transdermal film formulations of montelukast sodium with improved chemical stability and extended drug release, *Heliyon*, 2023, **9**, e14469, doi: 10.1016/j.heliyon.2023.e14469.

[25] R. Pereira, A. Tojeira, D. C. Vaz, A. Mendes, P. Bártolo, Preparation and characterization of films based on alginate and aloe vera, *International Journal of Polymer Analysis and Characterization*, 2011, **16**, 449-464, doi: 10.1080/1023666x.2011.599923.

[26] N. N. Daud, W. W. Jaafar, N. Ismail, R. Junin, M. A. Manan, A. K. Idris, Utilizing lignosulfonate from coconut husk as sacrificial agent to reduce surfactant adsorption, *IOP Conference Series: Earth and Environmental Science*, 2021, **765**, 012021, doi: 10.1088/1755-1315/765/1/012021.

[27] S. G. Reddy, Controlled release studies of hydroxychloroquine sulphate (hcq) drug-using biodegradable polymeric sodium alginate and lignosulphonic acid blends, *Rasayan Journal of Chemistry*, 2021, **14**, 2209-2215, doi: 10.31788/rjc.2021.1446508.

[28] M. Ge, Y. Li, C. Zhu, G. Liang, S. M. Jahangir Alam, G. Hu, Y. Gui, M. Junaebur Rashid, Preparation of organic-modified magadiite-magnetic nanocomposite particles as an effective nanohybrid drug carrier material for cancer treatment and its properties of sustained release mechanism by Korsmeyer-Peppas kinetic model, *Journal of Materials Science*, 2021, **56**, 14270-14286, doi: 10.1007/s10853-021-06181-w.

[29] G. Reddy S, Kinetic studies for the release of hydroxychloroquine sulphate drug (HCQ) In-vitro in simulated gastric and intestinal medium from sodium alginate and lignosulphonic acid blends, *Trends in Sciences*, 2023, **20**, 5318, doi: 10.48048/tis.2023.5318.

[30] X.-Z. Sun, G. R. Williams, X.-X. Hou, L.-M. Zhu, Electrospun curcumin-loaded fibers with potential biomedical applications, Carbohydrate Polymers, 2013, **94**, 147-153, doi: 10.1016/j.carbpol.2012.12.064.

[31] A. Rezaei, A. Nasirpour, H. Tavanai, M. Fathi, A study on the release kinetics and mechanisms of vanillin incorporated in almond gum/polyvinyl alcohol composite nanofibers in different aqueous food simulants and simulated saliva, *Flavour and Fragrance Journal*, 2016, **31**, 442-447, doi: 10.1002/ffj.3335.